Accurate modeling of amorphous Indium-Gallium-Zinc-Oxide TFTs deposited on plastic foil

Matteo Ghittorelli, Fabrizio Torricelli, Zsolt Miklos Kovács-Vajna, and Luigi Colalongo
Department of Information Engineering
University of Brescia
25123 Brescia, Italy
Email: m.ghittorelli@unibs.it

***Abstract*—Amorphous Indium Gallium Zinc Oxide (a-IGZO) thin-film transistors (TFTs) are widely used in backplanes of high-definition displays thanks to the high field effect mobility of a-IGZO. To design high-performances and high-functionality a-IGZO circuits accurate physical modeling is required. In this work we propose a physically based analytical model of the drain current of a-IGZO TFTs. Both trapped and free charge are accounted for, and according to many experimental observations the charge transport is described by multiple trapping and release (MTR). The model is compared with both measurements of TFTs fabricated on flexible substrate and numerical simulations, showing negligible error. The resulting mathematical expressions are suitable for computer-aided design implementation and for process characterization.**

I. Introduction

Amorphous oxide semiconductors (AOSs) thanks to their large electron mobility (>10 cm^2 V^{-1} s^{-1}), mechanical flexibility, optical transparency, ink-jet printing and near to room temperature deposition [1][2][3][4] are very promising materials for thin-film transistors (TFTs) technology. Among AOSs, amorphous Indium Gallium Zinc Oxide (a-IGZO) TFTs have already found application in the backplanes of flexible high-definition displays [5], sensors [6][7], memories [8] and high complexity circuits [9][10]. The development of such applications needs physical modeling and accurate understanding of the transistor electrical characteristics.

The electron transport path is very efficient because the conduction band of a-IGZO is composed of spherical overlapping orbitals, which is less sensitive to the arrangement of atoms [5]. Furthermore, the spherical geometry leads to a reduced density of localized states, which in a-IGZO is typically 10^{18} cm^{-3} eV^{-1}, about two order of magnitude lower than amorphous covalent semiconductors [11]. Accordingly, in a-IGZO TFTs is easy to push the Fermi energy level toward the mobility band and the charge transport depends on the interplay of both trapped and free charges [12].

Charge transport in a-IGZO TFTs is governed by multiple trapping and release (MTR) [13][14]: the carriers moving in delocalized states interact with the localized states through trapping and thermal release. The DOS shape is therefore of paramount of importance. The tail states are commonly approximated by an exponential function [12], [15], [16], [17], [18], while the deep states affect only the transistor threshold voltage [12][19] since they are of the order of $10^{13} \sim 10^{14}$ cm^{-3} and become filled when the gate voltage exceeds the flatband voltage of few tens of millivolts.

In this work, we propose an analytical model for a-IGZO TFTs that accounts for both the trapped and the free charges. It is compared with numerical simulations and experimental data collected from transistors fabricated on a flexible substrate. The model is physically based and enables a detailed discussion of the relative importance of localized and delocalized carriers. Furthermore, it can be exploited for physical parameters extraction and, thanks to the analytical formulation it can also be used for CAD implementation and process characterization.

This paper is organized as follows. In Section II, transistor fabrication is described. In Section III, the drain current model is derived and it is validated with respect to numerical simulations. In Section IV the model is validated with the measurements and the physical parameters are discussed. In Section V, conclusions are drawn.

II. Device Fabrication

The transistors are based on a bottom-contact (BC) bottom-gate (BG) structure (Fig. 1). The transistors are fabricated on a flexible substrate [25 μm polyethylene naphthalate (PEN)]. The foils were glued to a rigid carrier support (Si wafer) during fabrication and detached after processing. The gate were deposited by e-beam evaporation of gold with a thickness of 30 nm. 100-nm thick $Al_2 0_3$ gate insulator were formed by atomic layer deposition. The source and drain contacts were made by 5-nm thick e-beam evaporation of titanium and a 30-nm thick evaporation of gold. The 30-nm thick a-IGZO semiconducting layer were deposited by RF magnetron sputtering. All layers were patterned by means of a standard photolithographic process. Transistors with different channel lengths ranging from 5 to 100 μm and a channel width of 1 mm were fabricated [20].

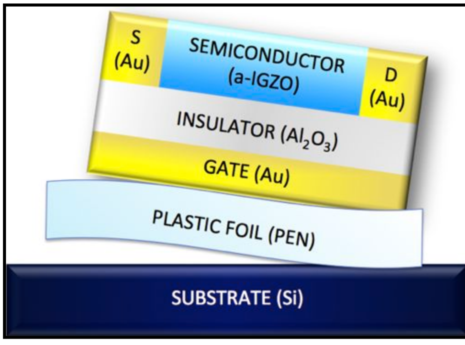

Fig. 1. Schematic cross section of the a-IGZO TFT coplanar structure.

III. Drain Current Model

The integral expression of the drain current reads [21]:

$$I_D = \frac{W}{L}\int_{V_S}^{V_D}\int_{V_{ch}}^{\varphi_s}\frac{\sigma(\varphi, V_{ch})}{F_x(\varphi, V_{ch})}d\varphi dV_{ch} \quad (1)$$

where W is the device width, L is the channel length, V_S and V_D are the source and the drain voltages, respectively, V_{ch} is the channel potential (quasi Fermi potential), φ the electrostatic potential and φ_s is the surface potential at the insulator-semiconductor interface. In order to evaluate the right-hand side of Eq. 1, the conductivity σ and the vertical electric field F_x in the accumulation layer should be expressed as a function of the electrostatic potential φ and of the channel voltage V_{ch}.

As shown in [12][19], the shape and the total number of the deep states affects only the threshold voltage, therefore the DOS is approximated as a tail exponential function:

$$g_t(E) = \frac{N_t}{E_t}\exp\left(\frac{E-E_c}{E_t}\right) \quad (2)$$

where N_t is the total number of localized states, $E_t = k_B T_t$, T_t is the characteristic temperature of the tail states, k_B is the Boltzmann constant; E_c is the conduction-band edge, which is assumed as the energy reference: $g_t(E) = 0$ at $E > E_c$. Accordingly, the MTR conductivity of a-IGZO semiconductor reads [21]:

$$\sigma = \sigma_0 \exp\left(\frac{\varphi - V_{ch}}{E_f}\right) \quad (3)$$

where $\sigma_0 = q\mu_0 N_f \exp(\Delta E_{Fi}/E_f)$; $E_f = k_B T$, μ_0 is the band mobility, N_f is the number of states per unit volume in the transport band, and $\Delta E_{Fi} = E_{gap}/2$. The electric field in the x-direction $F_x(\varphi, V_{ch})$, calculated by means of the Poisson equation is $\nabla^2\varphi = -(\partial F_x/\partial x + \partial F_y/\partial y)$ and assuming the gradual channel approximation (i.e. $F_x \gg F_y$) [21], reads:

$$F_x(\varphi, V_{ch}) = \sqrt{\frac{2q}{\epsilon_s}\int_{V_{ch}}^{\varphi} n(\varphi', V_{ch})d\varphi'} \quad (4)$$

$$\simeq \sqrt{k_f e^{\frac{\varphi - V_{ch}}{E_f}} + k_t e^{\frac{\varphi - V_{ch}}{E_t}}} \quad (5)$$

where ϵ_s is the a-IGZO semiconductor permittivity, $n = n_t + n_f$ is the total charge carrier concentration, n_t is the trapped charge concentration, n_f is the free charge concentration, $k_f = \frac{2qN_f E_f}{\epsilon_s}$, and $k_t = \frac{2qN_t E_t}{\epsilon_s}\frac{\pi T/T_t}{\sin(\pi T/T_t)}$.

Replacing Eq. 3 and Eq. 5 in Eq. 1, the resultant equation hampers any analytical solution: we approximate the inner integral of Eq. 1 as:

$$\int_{V_{ch}}^{\varphi_s}\frac{\sigma_0 e^{(\varphi - V_{ch})/E_f}}{\sqrt{k_f e^{(\varphi - V_{ch})/E_f} + k_t e^{(\varphi - V_{ch})/E_t}}}d\varphi \simeq$$

$$\frac{\sigma_0 e^{(\varphi_s - V_{ch})/E_f}}{\sqrt{k_f\left(\frac{1}{2E_f}\right)^2 e^{(\varphi_s - V_{ch})/E_f} + k_t\left(\frac{1}{E_f} - \frac{1}{2E_t}\right)^2 e^{(\varphi_s - V_{ch})/E_t}}} \quad (6)$$

Eq. 6 is a continuous function that accurately approximates the integral in the whole energy range and not only in the asymptotic regions as in the conventional approaches to calculate the drain current of amorphous covalent semiconductors [22]. In fact, at low band bending ($\varphi_s - V_{ch}$), the concentration of free charges is negligible with respect to the trapped ones, at large band bending the free charges concentration is the major term, and the trapped charges is eventually a negligible constant. In the transition region (weak accumulation regime) the concentration of free and trapped charge are comparable, and the contribution of none of them can be neglected. In a-IGZO semiconductor, the transition region is wide and and its contribution to the drain current must be accurately accounted for.

In Fig. 2 we investigate the accuracy of the proposed approximation: it is compared with numerical simulations as a function of the gate voltage V_G and of the correlation index (T_t/T) that is a synthetic parameter that ranging from 1 to 3 spans the whole space of the DOS parameters. The impact of the trapped charge is readily visible on the transfer characteristics: as the width of the tail exponential DOS decreases the subthreshold slope increases, resulting in a performance improvement. For the whole range of gate voltages and DOS parameters the approximate integral function perfectly reproduces the numerical simulations. To further validate the accuracy of the proposed approximation, in Fig. 3 we report the percentage error as a function of the gate voltage V_G and of the correlation index (T_t/T). The error is below few percent in the whole space of gate voltages and DOS parameters.

By applying Gauss law to the insulator-semiconductor interface one obtains:

$$\frac{C_i}{\epsilon_s}(V_G - V_{fb} - \varphi_s) = F_x(\varphi_s, V_{ch}) \quad (7)$$

where C_i is the gate capacitance per unit area, V_G and V_{fb} are the gate and the flatband voltages, respectively. Substituting Eq. 5 in Eq. 7, and after straightforward manipulations one obtains:

$$dV_{ch} = -1 - \frac{\epsilon_s}{2C_i}\frac{\frac{k_t}{E_t}e^{\frac{\varphi_s - V_{ch}}{E_t}} + \frac{k_f}{E_f}e^{\frac{\varphi_s - V_{ch}}{E_t}}}{F_x(\varphi_s, V_{ch})}d(\varphi_s - V_{ch}) \quad (8)$$

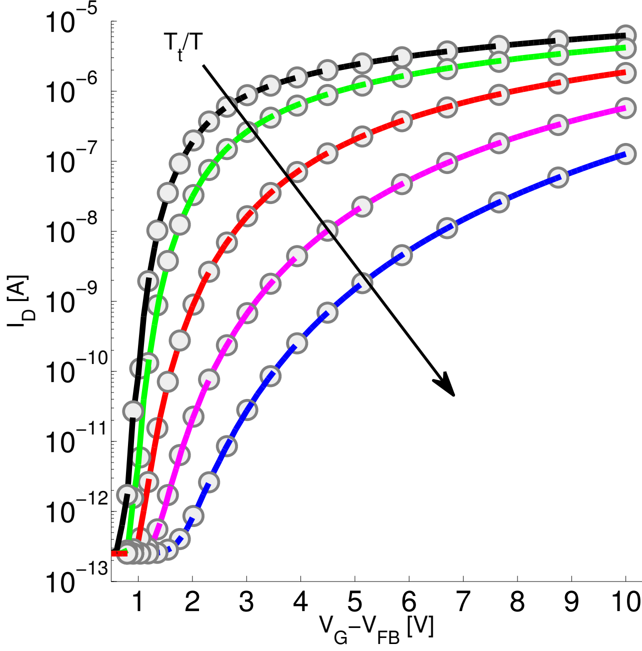

Fig. 2. Transfer characteristcs of a-IGZO TFT at $V_D = 1$ V as a function of the gate voltage ($V_G - V_{fb}$) and the trapped/free charge correlation index (T_t/T). Grey circles - exact numerical solution of Eq. 1, colored lines - numerical solution of Eq. 1 by introducing the analytical approximation (Eq. 6). The physical parameters are listed in Tab. I.

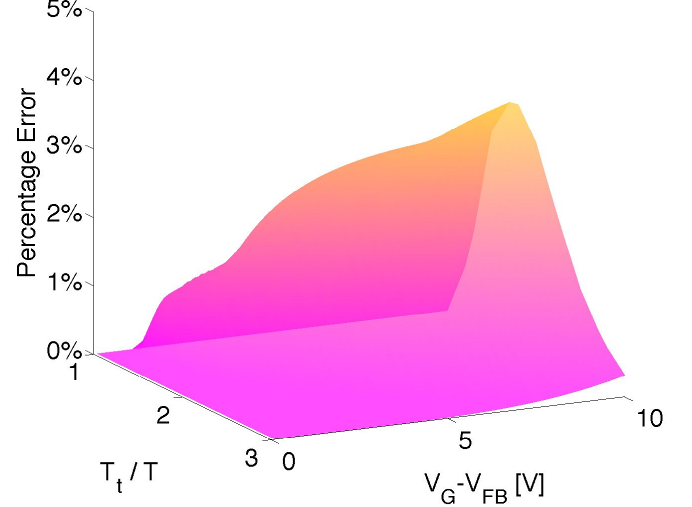

Fig. 3. Percentage error of numerical solution of Eq. 1, with respect to the numerical solution of Eq. 1 by introducing the analytical approximation (Eq. 6) as a function of the gate voltage ($V_G - V_{fb}$) and the trapped charge correlation index (T_t/T). The physical parameters are listed in Tab. I

The first term at the right hand side can be neglected if the gate voltage exceeds the flatband voltage of few tens of millivolts. Then, replacing Eq. 8 in Eq. 1 and changing the integration variable from V_{ch} to $\psi = \varphi_s - V_{ch}$ the drain current turns out to be:

$$I_D = \frac{W}{L}\beta \int_{\psi_D}^{\psi_S} \frac{\frac{k_f}{E_f} e^{\frac{\psi}{E_f}} + \frac{k_t}{E_t} e^{\frac{\psi}{E_t}}}{\sqrt{k + \gamma\, e^{\frac{\psi}{E_t} - \frac{\psi}{E_f}} + \lambda\, e^{\frac{2\psi}{E_t} - \frac{2\psi}{E_f}}}} d\psi \quad (9)$$

where $\psi_S = \varphi_{sS} - V_S$, $\psi_D = \varphi_{sD} - V_D$, φ_{sS} and φ_{sD} are the surface potential calculated at the source and the drain contact, respectively, and, the physical and geometrical parameters reads:

$$\beta = \frac{\epsilon_s \sigma_0}{2C_i} \quad ; \quad k = \frac{k_f^2}{4E_f^2} \quad ; \quad \lambda = \left(\frac{k_t}{E_f} - \frac{k_t}{2E_t}\right)^2$$

$$\gamma = k_f k_t \left(\frac{3}{2E_f^2} - \frac{1}{E_f E_t} + \frac{1}{4E_t^2}\right)$$

Finally, using the same approximation exploited in Eq. 6 to calculate the integral of Eq. 9, the drain current reads:

$$I_D = [I_{dF}(\psi_S) + I_{dT}(\psi_S)] - [I_{dF}(\psi_D) + I_{dT}(\psi_D)] \quad (10)$$

where I_{dF} and I_{dT} are defined as follow:

$$I_{dF}(\psi) = \frac{W}{L}\beta \frac{\frac{k_f}{E_f} e^{\frac{\psi}{E_f}}}{\sqrt{K_F + \Gamma_F\, e^{\frac{\psi}{E_t} - \frac{\psi}{E_f}} + \Lambda_F\, e^{\frac{2\psi}{E_t} - \frac{2\psi}{E_f}}}} \quad (11)$$

$$I_{dT}(\psi) = \frac{W}{L}\beta \frac{\frac{k_t}{E_t} e^{\frac{\psi}{E_t}}}{\sqrt{K_T + \Gamma_T\, e^{\frac{\psi}{E_t} - \frac{\psi}{E_f}} + \Lambda_T\, e^{\frac{2\psi}{E_t} - \frac{2\psi}{E_f}}}} \quad (12)$$

and:

$$K_F = \frac{k}{E_f^2}; \; \Gamma_F = \gamma \left(\frac{3}{2E_f} - \frac{1}{2E_t}\right)^2; \; \Lambda_F = \lambda \left(\frac{2}{E_f} - \frac{1}{E_t}\right)^2$$

$$K_T = \frac{k}{E_t^2}; \; \Gamma_T = \frac{\gamma}{4}\left(\frac{1}{E_f} + \frac{1}{E_t}\right)^2; \; \Lambda_T = \frac{\lambda}{E_f^2}$$

Eq. 10 is the analytical expression of the drain current of an a-IGZO TFT as a function of the applied external voltages (V_G,V_S, and V_D) and of the band bending calculated at the source and the drain contact (ψ_S and ψ_D) that in turn are functions of the external voltages as well. It accounts for both free and trapped charges; it is worth noting that both I_{dF} and I_{dT} depend on free and trapped charges but the analysis of the relative importance of each term shows that the current I_{dF} is manly driven by the free charge, while I_{dT} manly accounts for the trapped ones.

In Fig. 4 we show that in weak accumulation (i.e. small V_G), I_{dF} is negligible and the drain current is basically defined by the trapped charge I_{dT}. At large V_G, I_{dT} is roughly constant and the drain current is basically shaped by free charges I_{dF}. The surface potential and eventually the band bending ($\psi =$

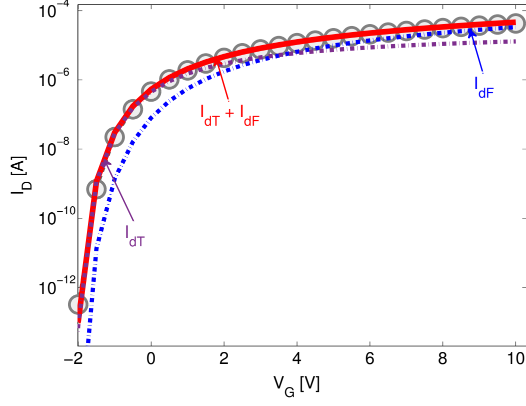

Fig. 4. Transfer characteristic of a-IGZO TFT at $V_D = 1V$. Grey circles are the numerical solution of Eq. 1, red line is the analytical model (Eq. 10). The violet dot-dashed line is the current due to the trapped charges only (Eq. 12) while the blue dot-dashed line is the current due to free charges only (Eq. 11). Parameters are shown in Tab. I.

TABLE I
TECHNOLOGICAL, GEOMETRICAL AND PHYSICAL PARAMETERS OF THE TRANSISTORS. W: TRANSISTOR WIDTH; L: TRANSISTOR CHANNEL LENGHT; k_s: A-IGZO SEMICONDUCTOR DIELECTRIC CONSTANT; C_i: GATE-INSULATOR CAPACITANCE PER UNIT AREA; μ_0: INFINITE TEMPERATURE MOBILITY; V_{fb}: FLATBAND VOLTAGE; N_t: TOTAL NUMBER OF TAIL STATES; N_f: TOTAL NUMBER OF FREE CHARGE STATES; T_t: TAIL-STATE CHARACTERISTIC TEMPERATURE; T: DEVICE TEMPERATURE.

$W\ [\mu m]$	1000	$V_{fb}\ [V]$	-2.87
$L\ [\mu m]$	100→5	$N_t\ [cm^{-3}]$	2.7 $\times 10^{19}$
k_s	7.9	$N_f\ [cm^{-3}]$	2.5 $\times 10^{20}$
$C_i\ [nF/cm^2]$	70	$T_t\ [K]$	523
$\mu_0\ [cm^2/Vs]$	11.8	$T\ [K]$	293

$\varphi_s - V_{ch}$) can be calculated by replacing Eq. 5 in Eq. 7:

$$\frac{C_i^2}{\epsilon_s^2}(V_G - V_{fb} - V_{ch} - \psi)^2 = k_f \exp\left(\frac{\psi}{E_f}\right) + k_t \exp\left(\frac{\psi}{E_t}\right) \quad (13)$$

IV. RESULTS AND DISCUSSION

The model is compared with the measurements of a-IGZO transistor in a wide range of bias conditions. In our transistor both trapped and free charges are relevant in a wide carrier energy range, and their relative influence must be accounted for also at large gate voltages. Physical parameters of the model are extracted at $V_D = 10V$. In such condition, the effect of parasitic contact resistance is minimized thanks to the coplanar structure [23]. As a consequence, a better estimation accuracy of the physical parameters can be achieved. Physical and geometrical parameters are listed in Tab. I. The comparisons between the measurements of transfer characteristics and the proposed model for a-IGZO TFT are shown in Fig. 5. There is a very good agreement between experimental data and model in the whole range of biasing conditions.

In Fig. 6 the output characteristics of a-IGZO TFT are shown. In both the linear and the saturation region the model is in good agreement with experimental data in the whole range of bias conditions. Finally, in Fig. 7 the L/W normalized

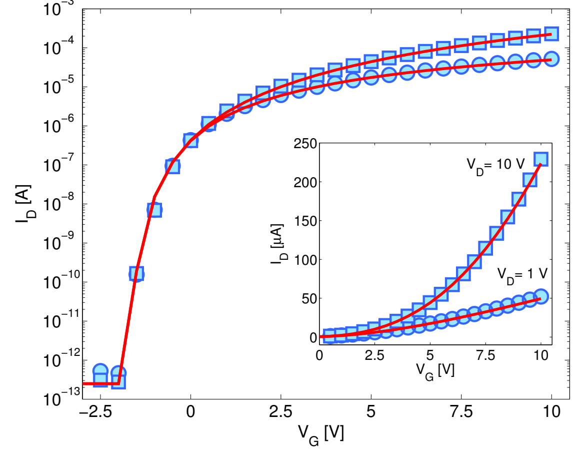

Fig. 5. Measured (blue symbols) and modeled (red lines) transfer characteristics of L=100μm a-IGZO TFT. The other geometrical and physical parameters are listed in Table I.

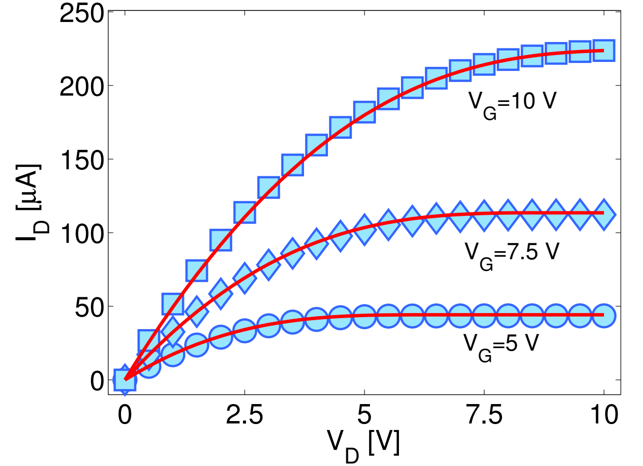

Fig. 6. Measured (blue symbols) and model (red lines) output characteristics of L=100μm a-IGZO TFT. The other geometrical and physical parameters are listed in Table I.

current of transistors with channel length ranging from $5\mu m$ to $100\mu m$ are shown. The model accurately reproduces the measured drain current also for the whole range of channel lengths.

V. CONCLUSION

An analytical model for a-IGZO TFTs has been proposed. The model is physically based and accounts for both trapped and free charges. The model is in very good agreement with the measurements of a-IGZO TFTs fabricated on flexible substrate. Thanks to the analytical formulation it is used in a CAD software for the design of high-functionality circuits. Furthermore, the model is suitable for the extraction of a-IGZO physical parameters and for technology characterization and improvement. The maximum error due to the approximations needed to obtain an analytical solution has been calculated by extensive numerical simulations and it is always lower than

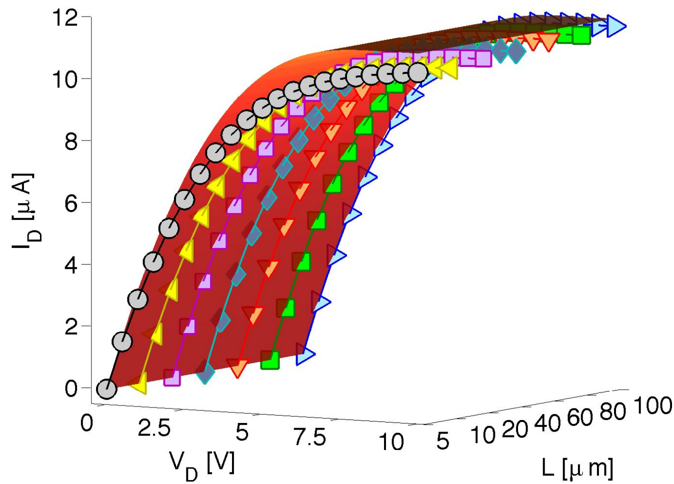

Fig. 7. Measured (colored lines with symbols) and modeled (red surface) L/W normalized output characteristics of a-IGZO TFTs at $V_G = 10V$. Geometrical and physical parameters are listed in Tab. I.

4%. Thanks to this, the physical parameters extraction results accurate. As a future work, to further improve the usability of the proposed model a surface potential analytical model that accounts for both trapped and free charges is desirable.

References

[1] K. Nomura, H. Ohta, A. Takagi, T. Kamiya, M. Hirano, and H. Hosono, "Room-temperature fabrication of transparent flexible thin-film transistors using amorphous oxide semiconductors," *Nature*, vol. 432, no. 7016, pp. 488-492, Nov. 2004.

[2] R. A. Street, Tse Nga Ng, R. A. Lujan, I. Son, M. Smith, S. Kim, T. Lee, Y. Moon, and S. Cho, "Sol-Gel Solution-Deposited InGaZnO Thin Film Transistors," *ACS Appl. Mater. Inter.*, vol. 6, no. 6, pp. 4428-4437, Mar. 2014.

[3] G. H. Kim, H. S. Kim, H. S. Shin, B. D. Ahn, K. H. Kim, and H. J. Kim, "Inkjet-printed InGaZnO thin film transistor," *Thin Solid Films*, vol. 517, no. 14, pp. 4007-4010, May. 2009.

[4] I. Song, S. Kim, H. Yin, C.-J. Kim, J. Park, S. Kim, H.-S. Choi, E. Lee, and Y. Park, "Short channel characteristics of gallium-indium-zinc-oxide thin film transistors for three-dimensional stacking memory," *IEEE Electron Device Lett.*, vol. 29, no. 6, pp. 549-552, Jun. 2008.

[5] T. Kamiya, K. Nomura, and H. Hosono, "Present status of amorphous In-Ga-Zn-O thin-film transistors," *Sci. Technol. Adv. Mater.*, vol. 11, no. 4, p.044305 , Aug. 2010.

[6] D.J. Yang, G.C. Whitfield, N.G. Cho, P.-S. Cho, I.-D. Kim, H.M. Saltsburg, and H.L. Tuller, "Amorphous InGaZnO4 films: gas sensor response and stability," *Sens. Actuators, B*, vol. 171-172, pp. 1166-1171, Aug. - Set. 2012.

[7] J. T. Smith, S. S. Shah, M. Goryll, J. R. Stowell, and D. R. Allee, "Flexible ISFET Biosensor Using IGZO Metal Oxide TFTs and an ITO Sensing Layer," *IEEE Sensors Journal*, vol. 14, no. 4, pp. 937-938, Apr. 2014.

[8] M. C. Chen, T. C. Chang, S. Y. Huang, S. C. Chen, C. W. Hu, C. T. Tsai, and S. M. Sze, "Bipolar resistive switching characteristics of transparent indium gallium zinc oxide resistive random access memory," *Electrochem. Solid State Lett.*, vol. 13, no. 6, pp. H191H193, Mar. 2010.

[9] A. K. Tripathi, E. C. P Smits, J. B. P. H. van der Putten, M.van Neer, K. Myny, M. Nag, S. Steudel, P. Vicca, K. ONeill, E. van Veenendaal, J. Genoe, P. Heremans, and G.H. Gelinck, "Low-voltage galliumindiumzincoxide thin film transistors based logic circuits on thin plastic foil: Building blocks for radio frequency identification application," *Appl. Phys. Lett.*, vol. 98, no. 16, pp. 162102-1 - 162102-3, Apr. 2011.

[10] D. Raiteri, F. Torricelli, K. Myny, M. Nag, B. Van Der Putten, E. Smits, S. Steudel, K. Tempelaars, A. Tripathi, G. Gelinck, A. Van Roermund, and E. Cantatore, "A 6b 10MS/s current-steering DAC manufactured with amorphous Gallium-Indium-Zinc-Oxide TFTs achieving SFDR > 30dB up to 300kHz," *ISSCC Dig. Tech. Pap. I.*, vol. 55, pp. 314-315, 2012.

[11] W. Körner, D. F. Urban, C. and Elsässer, "Origin of subgap states in amorphous In-Ga-Zn-O," *J. Appl. Phys.*, vol. 114, no. 16, pp. 163704-1 -163704-6, Oct. 2013.

[12] H. Hsieh, T. Kamiya, K. Nomura, H. Hosono, and C.Wu, "Modeling of amorphous $InGaZnO_4$ thin film transistors and their subgap density of states," *Appl. Phys. Lett.*, vol. 92, no. 13, pp. 133503-1 - 133503-3, Apr. 2008.

[13] S. Lee, K. Ghaffarzadeh, A. Nathan, J. Robertson, S. Jeon, C. Kim, I-H. Song, and U-I. Chung, "Trap-limited and percolation conduction mechanisms in amorphous oxide semiconductor thin film transistors," *Appl. Phys. Lett.*, vol. 98, no. 20, pp. 203508-1 - 203508-3, Mag. 2011.

[14] C-G. Lee, B. Cobb, and A. Dodabalapur, "Band transport and mobility edge in amorphous solution-processed zinc tin oxide thin-film transistors," *Appl. Phys. Lett.*, vol. 97, no. 20, pp. 203505-1 - 203505-3, Nov. 2010.

[15] K. Jeon, C. Kim, I. Song, J. Park, S. Kim, S. Kim, Y. Park, J.-H. Park, S. Lee, D. M. Kim, and D. H. Kim, "Modeling of amorphous InGaZnO thin-film transistors based on the density of states extracted from the optical response of capacitance-voltage characteristics," *Appl. Phys. Lett.*, vol. 93, no. 18, pp. 182102-1 - 182102-3, Nov. 2008.

[16] S. Lee, S. Park, S. Kim, Y. Jeon, K. Jeon, J.-H. Park, J. Park, I. Song, C. J. Kim, Y. Park, D. M. Kim, and D. H. Kim, "Extraction of Subgap Density of States in Amorphous InGaZnO Thin-Film Transistors by Using Multifrequency Capacitance-Voltage Characteristics," *IEEE Electron Device Lett.*, vol. 31, no. 3, pp. 231 - 233, Mar. 2010.

[17] Y. W. Jeon, S. Kim, S. Lee, D. M. Kim, D. H. Kim, J. Park, C. J. Kim, I. Song, Y. Park, U-I. Chung, J.-H. Lee, B. D. Ahn, S. Y. Park, J.-H. Park, and J. H. Kim, "Subgap Density-of-States-Based Amorphous Oxide Thin Film Transistor Simulator (DeAOTS)," *IEEE Trans. Electron Devices*, vol. 57, no. 11, pp. 2988-3000, Nov. 2010.

[18] Y. Kim, M. Bae, W. Kim, D. Kong, H. K. Jeong, H. Kim, S. Choi, D. M. Kim, and D. H. Kim, "Amorphous InGaZnO Thin-Film Transistors - Part I: Complete Extraction of Density of States Over the Full Subband-Gap Energy Range," *IEEE Trans. Electron Devices*, vol. 59, no. 10, pp. 2689-2698, Oct. 2012.

[19] S. Y. Lee, D. H. Kim, E. Chong, Y. W. Jeon, and D. H. Kim, "Effect of channel thickness on density of states in amorphous InGaZnO thin film transistor," *Appl. Phys. Lett.*, vol. 98, no. 12, pp. 122105-1 - 122105-3, Mar. 2011.

[20] F. Torricelli, A. K. Tripathi, E. C. P. Smits, L. Colalongo, Z. M. Kovacs-Vajna, G. H. Gelinck, and E. Cantatore, "Analysis and Modeling of Amorphous InGaZnO (aIGZO) ThinFilm Transistors," *14th Workshop on Semiconductor Advances for Future Electronics*, Veldhoven, The Netherlands, Nov. 2011.

[21] F. Torricelli, J. R. Meijboom, E. C. P. Smits, A. K. Tripathi, M. Ferroni, S. Federici, G. H. Gelinck, L. Colalongo, Z. M. Kovcs-Vajna, D. M. de Leeuw, and E. Cantatore,"Transport Physics and Device Modeling of Zinc Oxide Thin-Film Transistors - Part I: Long-Channel Devices," *IIEEE Trans. Electr. Devices*, vol. 58, no. 8, pp. 2610-2619, Aug. 2011.

[22] L. Colalongo, "A new analytical model for amorphous-silicon thin-film transistors including tail and deep states," *Solid-State Electron.*, vol. 45, no. 9, pp. 1525-1530, Sep. 2001.

[23] J.J. Brondijk, F. Torricelli, E.C.P. Smits, P.W.M. Blom, and D.M. de Leeuw, "Gate-bias assisted charge injection in organic field-effect transistors," *Appl. Phys. Lett.*, vol. 13, no. 9, pp. 1526-1531, Sep 2012.